OPTIMIZATION OF DRILL GEOMETRY DESIGN TO MINIMIZE THERMAL NECROSIS IN SURGICAL BONE DRILLING

R. Izamshah, M.S. Noorazizi, M.S. Kasim, M. Hadzley, M.A. Ali and S.A Sundi

Precision Machining Group,
Faculty of Manufacturing Engineering,
Universiti Teknikal Malaysia Melaka,
Hang Tuah Jaya, 76100 Durian Tunggal, Melaka, Malaysia.

Corresponding Author's Email: izamshah@utem.edu.my

Article History: Received 4 August 2017; Revised 18 October 2017; Accepted 16 December 2017

ABSTRACT: During the orthopedic bone drilling surgery procedures, the friction between the drill and bones surface leads to a localized temperature increase results in thermal necrosis on the soft tissue surrounding the hole. The magnitudes of the friction energy are greatly dependent with the drill geometry design. Recognizing the importance on studying this phenomenon, this paper aim to investigate the effects of drill geometry on temperatures during the bone drilling procedure. Totals of 17 drills were design and tested with different geometry namely point angle, helix angle and web thickness on different penetration angle (0^0, 15^0, and 30^0) to mimic the manually control penetration by the surgeon. From the conducted investigation, the most significant parameter that affects the temperature rise was the penetration angle followed by the point angle. In addition, the interaction between helix angle and web thickness also controlled the drilling temperature. From the result, the optimum drill-bit design geometry was 21.8% web thickness, 126.92° point angle and 36.53° helix angle which produces the minimum drilling temperature.

KEYWORDS: *Bone Drilling; Surgical Drill; Thermal Necrosis*

1.0 INTRODUCTION

One of the principal methods for repairing and reconstruction of a bone fracture are achieved by drilling the bone and fixing the separate parts together using screws, wires and plates. Many problems are encountered with the bone drilling process such as holes accuracy, drill wander and excessive heat generation which were directly related with the drilling parameter [1-2]. Many different drill-bit designs and geometries have been suggested over the years each with its own promising results [3-6]. However, most of the studies neglected the effects of penetration angle on the drilling performances. Generally, in normal orthopedic surgery, bone drilling is performed using hand drills and the penetration angles are greatly dependent on the surgeon's manual skill and are normally deviated from the normal axis.

Thermal necrosis is a common phenomenon during the bone drilling procedure due to the sensitivity of the soft tissue surrounding the bone [7]. Ideally, the generated drilling temperature must be below 47°C in order to avoid thermal necrosis [8-9]. The magnitude of the drilling temperature is greatly dependent with the drill geometry design [10-11] and should be methodically analyse to control the temperature rise.

2.0 EXPERIMENTAL WORKS

In this experiment, AISI 420B stainless steel medical grade rod with diameter 4.3 mm were ground to form the drill bits with varying angles namely point angle, helix angle and web thickness as depicted in Table 1. Stainless steel drill bit exhibits good corrosion resistance and can minimize the tool wear effect [12]. Totals of 51 holes were drilled with 3 holes replication for each run. To eliminate the apparatus wear impact on the result, the apparatus were cleaned with a brush and wet tissue before each drilling process.

Table 1: Drill geometrical angles design level

	Name	unit	low	high
A	Web Thickness	%	14	32
B	Point Angle	º	90	140
C	Helix Angle	º	16	38
D	Cutting Angle	º	0	30

Bovine cortical femur bone was chosen as the work material due to its closeness properties and characteristics with human bone [14]. Table 2 shows the mechanical properties of bovine femur. Fresh cortical (compact bone) samples are cuts and mills from bovine femur with a uniform thickness of 4 mm as shown in Figure 1.

Table 2: Mechanical properties of bovine femur

Mechanical properties	Value
Density (kg/m3)	1800
Young's modulus (MPa)	20000
Longitudinal elastic modulus (GPa)	26.1
Transverse elastic modulus (GPa)	10.9
Longitudinal tensile strength (MPa)	140
Transverse tensile strength (MPa)	46
Poisson's ratio	0.36

The drilling tests were performed using a DMU60 mono BLOCK DECKEL MAHO CNC 5-Axis Machine. The drilling speed of 1000 rpm and 100 mm/min feed rate were employed to represent the actual manual surgical hand drills speed and surgeon penetration feed. The drilling temperature was measured using portable thermal infrared camera Thermal Cam FlirOne. The camera was positioned so as not to interfere with the drilling process and simultaneously take full advantage of the environment and light available. To minimize the noise and external interference the measurement distance, environmental conditions and lighting conditions were kept constant for all the runs [15]. The accurate temperature measurement using infrared techniques requires knowledge of the emissivity that is the relationship between the amounts of infrared radiation emitted by a surface relative to a black body. This property is of great importance, as it incorporates a direct way to quantify the energy emitted by the bone. In this study the value of emissivity was set to 0.98. Figure 2 shows the detail of the experimental setup.

3.0 RESULTS AND DISCUSSION

The effects of drill geometries such as point angle, web thickness and helix angle contribute significantly on the temperature rise. From the conducted experimental tests, it is evidently shows the variation of drilling temperature for different drills design as well with the variation of penetration angle. Table 3 shows the experimental results for all the runs. From the result, the minimum drilling temperature obtained was 28 °C from drill design no. 16 at 0° penetration angle condition.

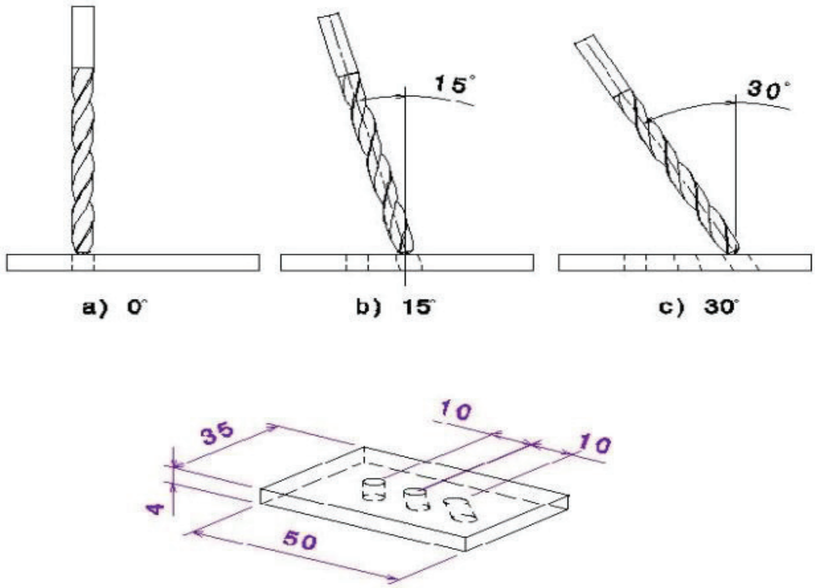

Figure 1: Bone work-piece with its drilling cutting for angles 0^0, 15^0 and 30^0

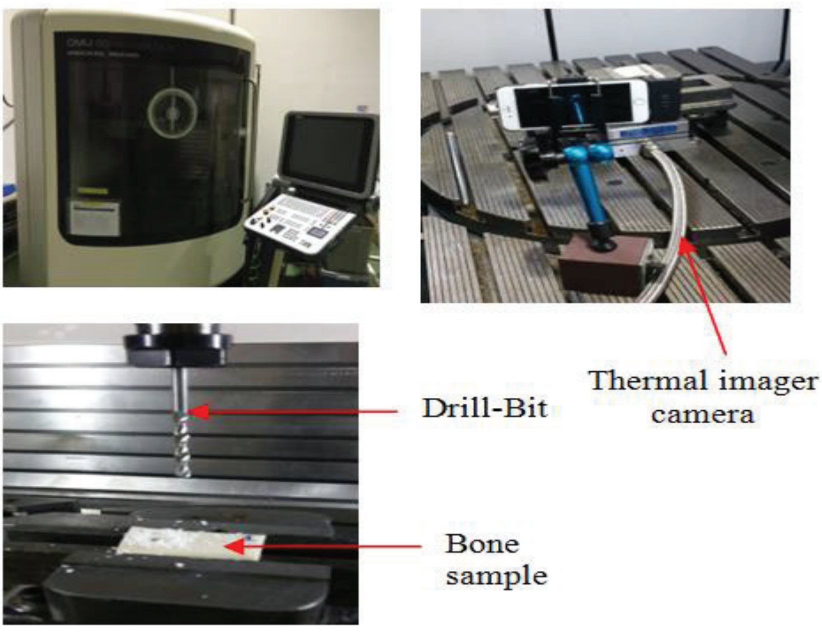

Figure 2: Experimental setup

The highest recorded temperature was 62.2 °C for drill design no. 44 at 30° penetration angle condition. Figures 3 and 4 show the screenshot of the minimum and maximum recorded temperatures.

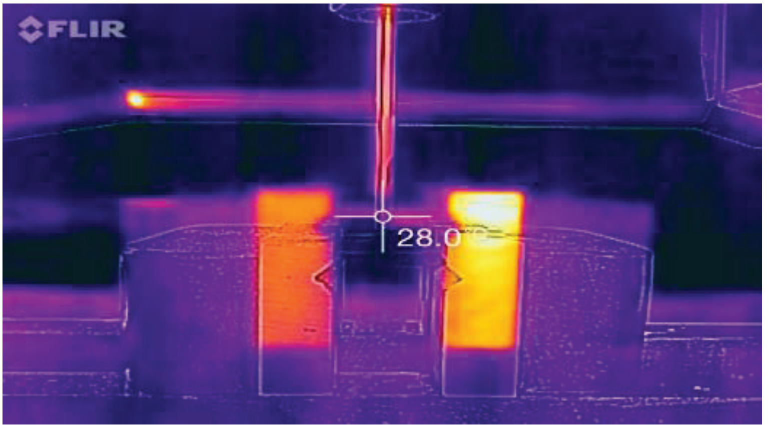

Figure 3: Minimum recorded temperature for run no. 16

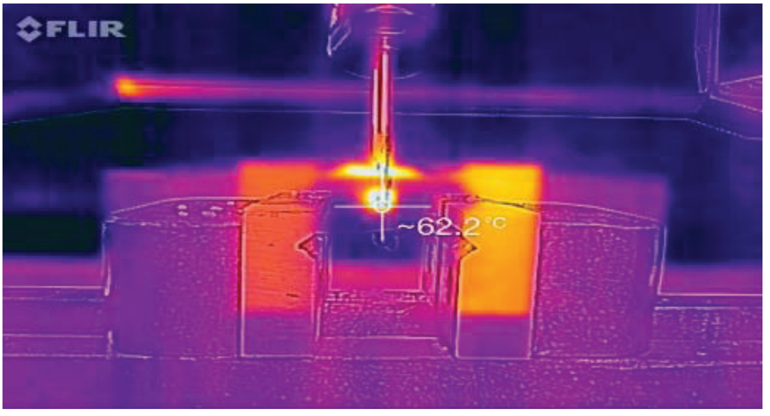

Figure 4: Maximum recorded temperature for run no. 44

Based on the obtained result, analysis of variance (ANOVA) was perform to predicted the response surface model on the influence of web thickness, point angle, helix angle and drilling angle for a confidence level of 95% as shown in Table 4. Based on the ANOVA, a mathematical quadratic function model of the temperature correlated with the drill design parameter was found to be significant with a P-value of less than 0.05. The design geometry parameters with P-values of less than 0.05 indicated that the model terms significantly affected the response in the design space.

Equation (1) shows the correlation between the temperature and the drill design geometry parameters, i.e. web thickness, point angle, helix angle and cutting angle. The prediction model can be denoted by the equation as:

$$\text{Temp } (C°)^{-1.69} = -0.018 + 3.52 \times 10^{-4}A + 3.64 \times 10^{-4}B - 2.83 \times 10^{-4}C - 1.01 \times 10^{-4}D + 6.63 \times 10^{-7}AB - 1.53 \times 10^{-6}BC + 2.38 \times 10^{-6}AD + 3.47 \times 10^{-7}BC + 1.27 \times 10^{-7}BDC^2 + 1.27 \times 10^{-7}CD - 8.33 \times 10^{-6}A^2 - 1.68 \times 10^{-6}B^2 - 5.39 \times 10^{-6} \quad (1)$$

The above mathematical model can be used to predict the values of the temperature within the limits of the factors studied. In Figure 5, the 3D response surface plots show the effect of drill geometry parameters on the temperature at different drilling angle, respectively. The graphs denote the temperature with respect to two different parameters by keeping the third parameter constant at the middle level. It can be stated that the temperature increases with an increasing in the drilling penetration angle and the increases of point angle whereas the web thickness and helix angle at the middle level generate the lowest temperature.

Table 3: Experimental result

Run	We	Point	Helix	Drilling	Temp.	Run	Web	Point	Helix	Drilling	Temp.
1	23	115	27	0	31.2	27	32	90	27	15	58.4
2	14	140	27	0	41.6	28	23	115	27	15	31.3
3	14	90	27	0	48	29	23	90	38	15	34.5
4	23	115	27	0	35	30	32	115	38	15	30.1
5	14	115	16	0	33.1	31	23	90	16	15	32.4
6	23	115	27	0	31	32	23	115	27	15	29.5
7	14	115	38	0	31	33	23	140	16	15	59
8	23	140	38	0	30.8	34	32	115	16	15	28.8
9	32	140	27	0	49	35	23	115	27	30	39.1
10	32	90	27	0	58	36	14	140	27	30	35
11	23	115	27	0	29.1	37	14	90	27	30	30.6
12	23	90	38	0	28	38	23	115	27	30	43.9
13	32	115	38	0	28.8	39	14	115	16	30	45.1
14	23	90	16	0	35	40	23	115	27	30	31.7
15	23	115	27	0	28.8	41	14	115	38	30	35.6
16	23	140	16	0	28	42	23	140	38	30	33.5
17	32	115	16	0	29	43	32	140	27	30	35.8
18	23	115	27	15	29.3	44	32	90	27	30	62.2
19	14	140	27	15	64.2	45	23	115	27	30	32.4
20	14	90	27	15	29.5	46	23	90	38	30	37.6
21	23	115	27	15	40.4	47	32	115	38	30	31.2
22	14	115	16	15	40.2	48	23	90	16	30	48.7
23	23	115	27	15	30.9	49	23	115	27	30	30.5
24	14	115	38	15	36.7	50	23	140	16	30	58.8
25	23	140	38	15	33.2	51	32	115	16	30	30.1
26	32	140	27	15	50.7						

Table 4: ANOVA Result

Source	Mean Square	F Value	Prob > F	
Model	1.77E-06	6.245147	< 0.0001	significant
A-Web thickness	2.43E-06	8.588499	0.0060	
B-Point angle	6.42E-08	0.226565	0.6371	
C-Helix	1.22E-06	4.306202	0.0456	
D-Drilling angle	4.37E-06	15.41974	0.0004	
AB	1.76E-07	0.620749	0.4362	
AC	2.76E-07	0.974119	0.3306	
AD	1.34E-06	4.733851	0.0366	
BC	1.09E-07	0.386427	0.5383	
BD	3E-12	1.06E-05	0.9974	
CD	2.62E-07	0.924137	0.3432	
A^2	5E-06	17.67054	0.0002	
B^2	1.21E-05	42.83787	< 0.0001	
C^2	4.56E-06	16.09228	0.0003	
Residual	2.83E-07			
Lack of Fit	2.84E-07	1.00821	0.5137	not significant

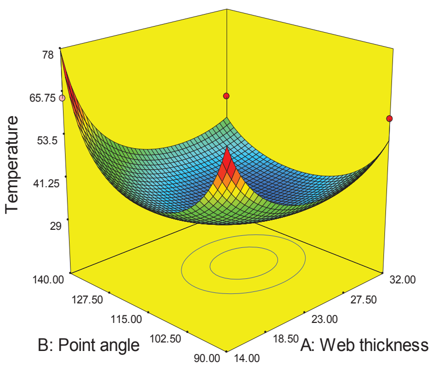

(a) Point angle and Web thickness

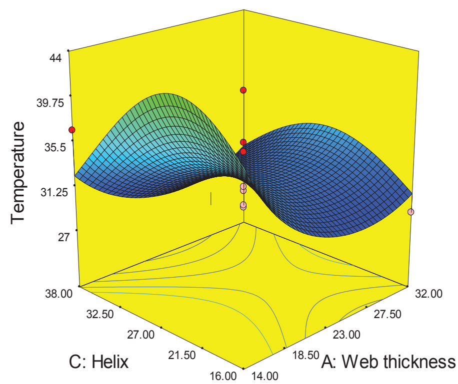

(b) Helix angle and Web thickness

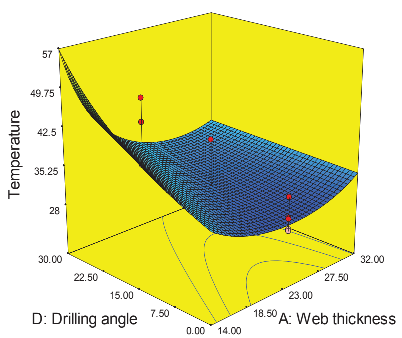

(c) Drilling angle and Web thickness

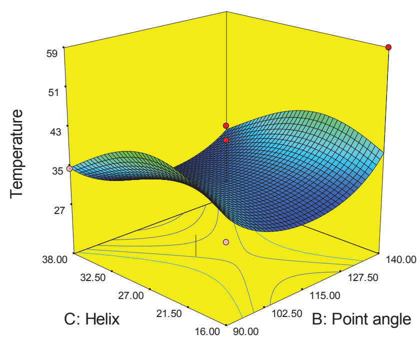

(d) Helix angle and Point angle

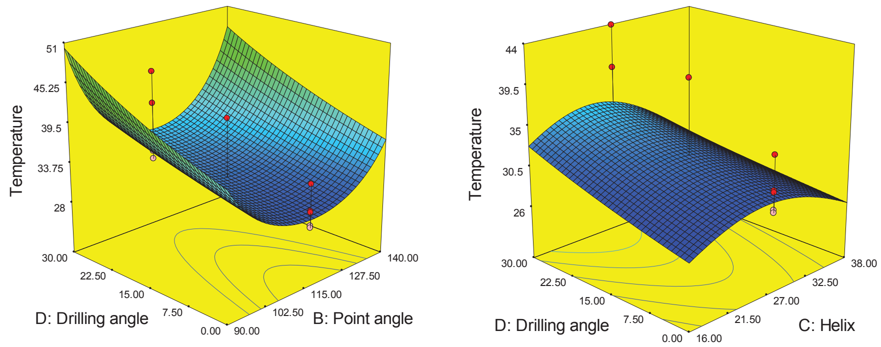

(e) Drilling angle and Point angle (f) Drilling angle and Helix angle

Figure 5: (a)-(f) 3D Response surface results on temperature vs drill geometry

Using the developed mathematical model of individual response correlated with the design geometry parameter, further analysis on the optimization was performed. The optimization processes aim on minimizing the drilling temperature for varied drilling angle condition based on combination of drill design parameters. Based on the desirability function, totals of three suggested scheduling values were generated with d = 0.9024, as shown in Table 5.

Table 5: Optimization result

Drill Geometry			Response	Desirability	
Web thickness	Point angle	Helix angle	Temp		
21.8	126.92	36.53	28	0.9024	Selected
21.78	126.5	36.41	27.99	0.9023	
22.01	126.78	36.46	27.99	0.9023	

Based on the selected optimized drill design, an additional identical set of experiments for all the drilling angles i.e. 0°, 15° and 30° were performed to validate the effectiveness of the model. The obtained temperatures for the tests were 28 °C, 29.7 °C and 31.64 °C for 0°, 15° and 30° respectively which confirmed the model validity and meets the safe drilling bone temperature requirement to avoid thermal necrosis on the soft tissue.

4.0 CONCLUSION

Practical investigations on the effects of drilling temperature with different drill geometry parameters were studied. The following conclusion can be drawn:

- This study demonstrated the interaction on the effects of drill-bit design geometry parameters with temperature for different drilling angle conditions. The interaction between the design geometry parameter and the drilling angle significantly affect the temperature magnitudes.

- From the result, the optimized drill-bit design geometry was 21.8% web thickness, 126.92° point angle and 36.53° helix angle produces the minimum temperature to avoid the thermal necrosis.

- To conclude, the results from the conducted experiments provide the reference values for the development of high performance surgical drill design in orthopedic bone surgeries application.

ACKNOWLEDGMENTS

The authors would like to thank to the Faculty of Manufacturing Engineering, Universiti Teknikal Malaysia Melaka and the Government of Malaysia for the technical and financial support for the experiment under Scholarship HLP (Hadiah Latihan Persekutuan).

REFERENCES

[1] T. Udiljak, D. Ciglar, and S. Skoric, "Investigation into bone drilling and thermal bone necrosis", *Advanced Production Engineering and Management*, vol. 2, pp. 103–112, 2007.

[2] K. Alam, M. Khan, R. Muhammad, SZ, Qamar, and V.V.Silberschmidt, "In-vitro experimental analysis and numerical study of temperature in bone drilling," *Technology and Health Care*, vol. 23, no.6, pp. 775-783, 2015.

[3] M.T. Hillery and I. Shuaib, "The drilling of bone using guide wires and twist drills," IMC-13, Ireland, pp. 33-42, 1996.

[4] R. K. Pandey and S. S. Panda, "Drilling of bone: A comprehensive review," *Journal Clinical Orthopaedics and Trauma*, vol. 4, no.1, pp. 15-30, 2013.

[5] T. Ueda, A. Wada, and K. Hasegawa, "Design optimization of surgical drills using the Taguchi method", *Journal Biomech Science Engineering*, vol. 5, no.5, pp. 603-614, 2010.

[6] R. Izamshah, M. A. Azam, M. Hadzley, M.A. Md Ali, M.S. Kasim, and M.S. Abdul Aziz, "Study of surface roughness on milling unfilled-polyetheretherketones engineering plastics," *Procedia Engineering*, vol. 68, pp. 654-660, 2013.

[7] G. Augustin, T. Zigman, S. Davila, T. Udilijak, T. Staroveski, D. Brezak and S. Babic., "Cortical bone drilling and thermal osteonecrosis," *Clinical Biomechanics*, vol. 27, no.4, pp. 313-325, 2012.

[8] R. Eriksson and R. Adell, "Temperature during drilling for placement of implants using osseointegration technique," *Journal of Oral and Maxillofac Surgery*, vol. 44, no.1, pp. 4–7, 1986.

[9] M. B. Abouzgia and D. F. James, "Temperature rise during drilling through bone," *International Journal of Oral and Maxillofacial Implants*, vol. 12, no 3, pp. 342-353, 1997.

[10] M.A. Amran, S. Salmah, NIS Hussein, R. Izamshah, M. Hadzley, MS Kasim and M.A. Sulaiman, "Effects of machine parameters on surface roughness using response surface method in drilling process", *Procedia Engineering*, vol. 68, pp. 24-29, 2013.

[11] R. K. Pandey and S. S. Panda, "Evaluation of delamination in drilling of bone," *Medical Engineering and Physics*, vol. 37, no.7, pp. 657-664, 2015.

[12] S.A. Hussein, A.S.M. Tahir, and R. Izamshah, "Generated forces and heat during the critical stages of friction stir welding and processing," *Journal of Mechanical Science and Technology*, vol. 29, no.10, pp. 4319-4328, 2015.

[13] D. Vashishth, K.E. Tanner and W. Bonfield, "Contribution, development and morphology of microcracking in cortical bone during crack propagation," *Journal of Biomechanics*, vol 33, pp. 1169-1174, 2000.

[14] Z. Liao and D. A. Axinte, "On monitoring chip formation, penetration depth and cutting malfunctions in bone micro-drilling via acoustic emission," *Journal of Materials Processing Techonolgy*, vol. 229, pp. 82-93, 2016.

[15] Y Hu, Q Zhang, and X Yue, "Study on the prediction of drilling forces on cortical bone based on finite element simulation", *Key Engineering Material*, vol. 589, pp. 157–162, 2014.